41st Aerospace Sciences Meeting and Exhibit
6-9 January 2003, Reno, Nevada

AIAA 2003-349

AERODYNAMIC CHARACTERISTICS OF THE LS(1)-0417MOD AIRFOIL MODEL

Jolanta M. Janiszewska, Gerald Gregorek and John Lee
Aeronautical and Astronautical Research Laboratory at The Ohio State University
2300 W. Case Rd., Columbus, Ohio 43235
janiszewska.1@osu.edu; gregorek.1@osu.edu; lee.30@osu.edu

ABSTRACT

The LS(1)-0417MOD airfoil model was tested in The Ohio State University's 3x5 wind tunnel both clean and with the application of leading edge grit roughness and with vortex generators. The tests were conducted in both two-dimensional and three-dimensional model configurations and for steady state and unsteady flow conditions. Pressure data were obtained from six spanwise stations. The results showed that the application of the grit roughness reduces the maximum lift coefficients in all configurations. Unsteady maximum lift coefficients were always higher than those for steady state and had, generally, large hysteresis loops. In the case of the unsteady flow however, the hysteresis loops were smaller for the three dimensional (wing) flows. The smallest hysteresis loops were found at the tip spanwise station. The application of the vortex generators at certain chordwise locations reduced the hysteresis loops and increased the maximum lift coefficient, especially in the three dimensional configuration.

INTRODUCTION

An understanding of the unsteady flow behavior around the wind turbine rotor is helpful in the design of new rotors with less sensitive characteristics. Horizontal axis wind turbine rotors experience unsteady aerodynamics due to the wind shear while the rotor is yawed, when the rotor blades pass through the support tower wake or during atmospheric turbulence. Wind tunnel experiments, which use a two dimensional model provide the main characteristics of the unsteady phenomena. The unsteady characteristics of an actual wing are much more complex, since they include the tip vortex effects and tapered and twisted wing effects. A simple simulation of a wind turbine blade uses a constant chord wing model to explore the effects of the tip vortex.

Additionally, the rotors experience performance degradation due to the surface irregularities, which occur because of the accumulation of insect debris or ice and the aging of the blades. The performance degradation due to the roughness can be minor or severe depending on the airfoil shape and degree of contamination.

Vortex generators on the surface of the blades have the potential to reduce the effects of the flow degradation and/or unsteady effects through their ability to bring higher momentum flow into the lower portion of the boundary layer, thereby delaying stall and increasing the maximum lift coefficient with a minor increase in drag.

Wind tunnel studies ,which examine both the steady state and unsteady flow characteristics for both two-dimensional and three-dimensional configurations of airfoils, define the pertinent flow phenomena. The resultant data may be used to gain a better understanding of the flow fields and to validate analytical codes. The research deals with the LS(1)-0417MOD airfoil profile and includes tests with a clean model and with the application of leading edge grit roughness (LEGR). It was tested in a two-dimensional (2D) configuration and a three-dimensional (3D) configuration having a semispan aspect ratio of 3.3. Pitch oscillations with a sine forcing function cam were used to establish the unsteady flow field .

EXPERIMENTAL SETUP

The Ohio State University (OSU) 3x5-foot wind tunnel was used to conduct the tests of the LS(1)-0417MOD airfoil model. This is an open circuit wind tunnel with a velocity range of 0-50 m/s (180 ft/s). The model had an 45.7cm (18 inch) chord and was mounted vertically in the test section. Tests for 2D and 3D were performed at 0.75, 1.00 and 1.25 million Reynolds numbers for both steady

state and unsteady flow conditions.

Airfoil Model

The airfoil model was made in four sections, where only one section was instrumented with two rows of pressure taps, a total of 76 taps (see figure 1). The hatch built into this section allowed for short lines from the taps to PSI modules (Pressure System Incorporated measuring system), to minimize the response time for the unsteady testing. Only the instrumented section was securely bonded to the support shaft, while the other sections were interchangeable, making it possible to measure the pressures distributions at six different locations across the span. The fourth piece was manufactured to extend the model for 2D baseline testing.

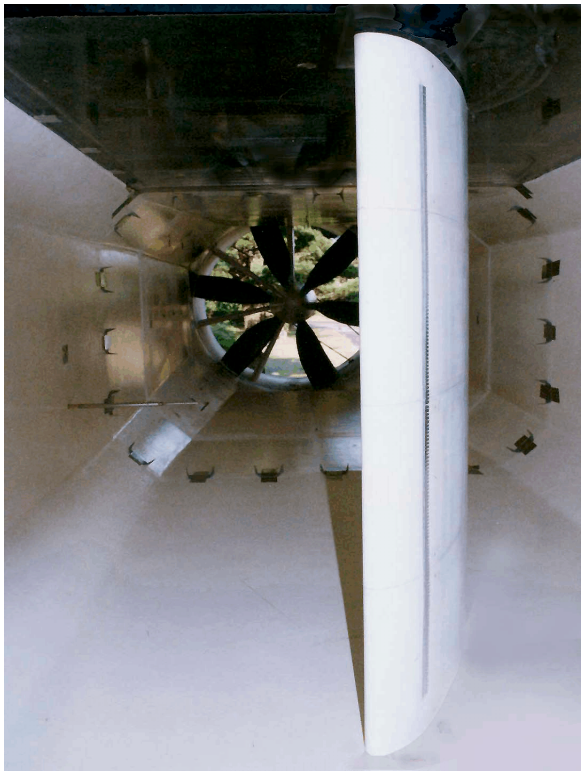

Figure 1. LS(1)-0417MOD airfoil model.

For tests involving leading edge grit roughness (LEGR) a standard pattern templet was used; this pattern was generated using a molded insect pattern taken from a wind turbine in the field. To simulate the pattern, #40 lapidary grit was applied, giving k/c=0.0019. Double sided tape was then used to transfer the pattern to the model. Figure 2 shows the LEGR templet pattern, this produced a severe contamination on the model.

Drag was measured by probing the wake with a pitot-static probe for the steady state tests only where the wake was definable (for angles of attack from -10˚ to 10˚).

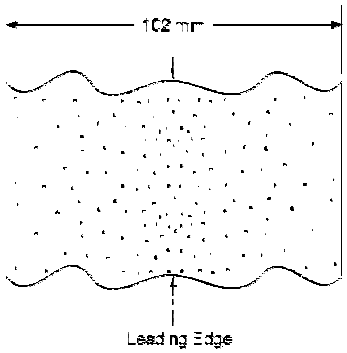

Figure 2. Leading edge grit roughness templet

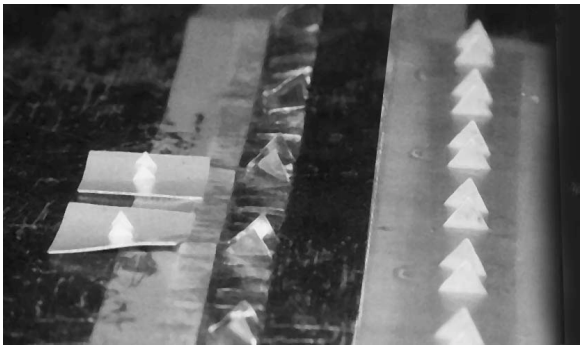

Figure 3. Sample of vortex generators.

Several different types of vortex generators were tried in an early exploratory study. Samples are shown in figure 3. Type A are shown on the far right and type B, a derivative of type A are next to them. Vortex generators were positioned at x/c from 0.07 to 0.5 in an attempt to determine optimum configurations and locations with regard to drag and maximum lift. Figure 4 shows the schematic of type A and type B vortex generators .

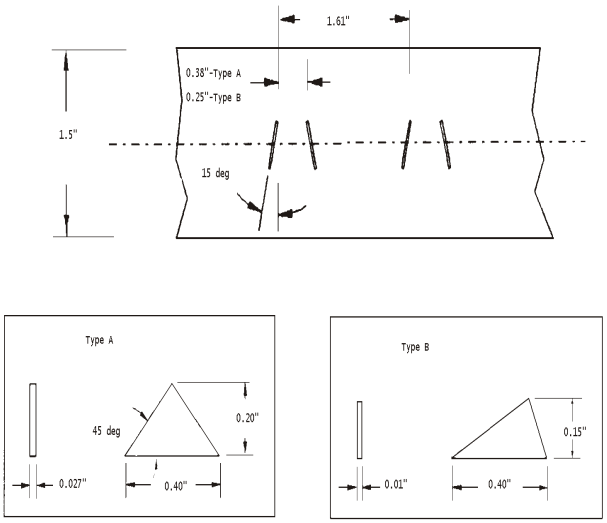

Figure 4. Schematic of the vortex generators.

Unsteady Setup

For the unsteady flow conditions the model was oscillated using a cam, the choice of which governs the type and amplitude of the wave forms produced. Sine waves with two different amplitudes, ±10˚ and ±5.5˚, were used. The data were taken for three frequencies of 0.6, 1.3, 1.8 Hz (correspond to the rotor RPM of 36, 78 and 108) and for three different mean angles of 8˚, 14˚ and 20˚. These particular mean angles were chosen because they cover the linear, the stall and deep stall angle of attack ranges.

RESULTS

Steady 2D Data

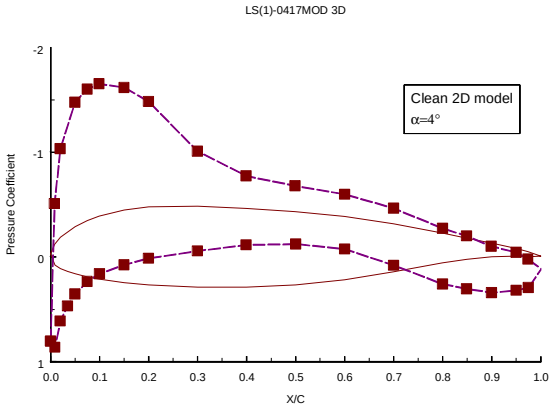

Figure 5. Typical pressure distribution and the airfoil profile.

A typical pressure distribution and the airfoil profile are shown in figure 5. The chosen pressure distribution is for clean airfoil in the 2D configuration at 4˚ angle of attack. The pressure distributions were integrated to obtain the lift, and pitching moment coefficient.

For the clean airfoil model the maximum lift coefficients occur almost at the same angle of attack and are almost equal for the tested Reynolds numbers of 0.75, 1.0, 1.25 million. The application of LEGR reduces the maximum lift coefficient and changes the lift curve slope slightly; typical results are shown in figure 6.

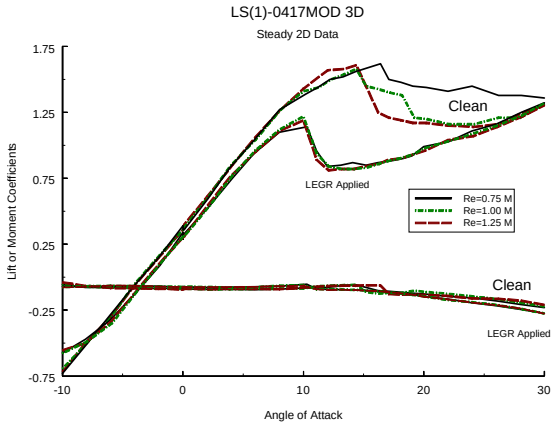

Figure 6. Comparison of clean and LEGR applied steady 2D lift and pitching moment coefficients.

For a Reynolds number of 1 million, the maximum lift coefficient for the clean model was 1.58 and with the LEGR it drops to 1.19, a 25% reduction. In addition, the lift curve slope changes from 0.113 (clean) to 0.089 with the LEGR applied. Typically, the pitching moment was only slightly affected by the presence of the LEGR. The wake drag was taken from -10˚ to 10˚ angle of attack and is shown in figure 7. As expected, the application of the LEGR consistently increased the drag; at 1 million, the minimum drag was 0.0086 for the clean model condition and 0.0138 for the LEGR, a 60% increase.

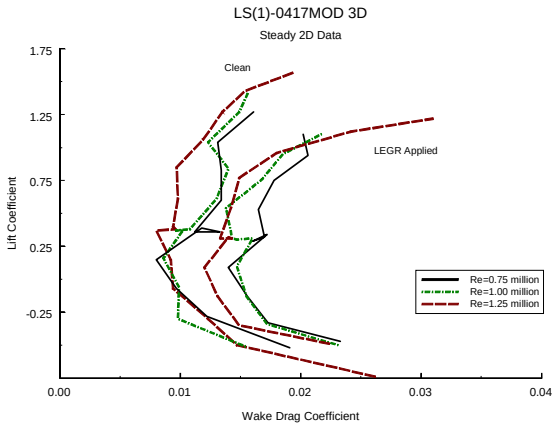

Figure 7. Comparison of clean and LEGR applied 2D wake drag coefficients.

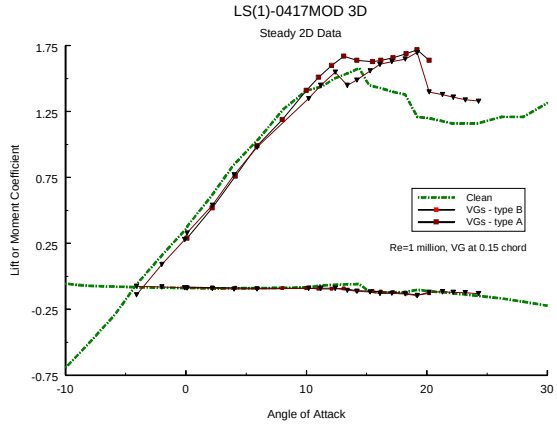

Figure 8. 2D steady lift coefficient with vortex generators.

From the many different configurations of the vortex generators, types A and B were the most successful with the results are shown in figure 8. The maximum lift coefficient increased with type B vortex generators and was maintained for more than 5˚. Runs with almost all types of vortex generators maintain the lift curve slope until stall whereas, by comparison, data from the clean model shows a departure at 10˚ angle of attack, approximately 5˚ before stall. The pitching moment is not affected by the application of the vortex generators.

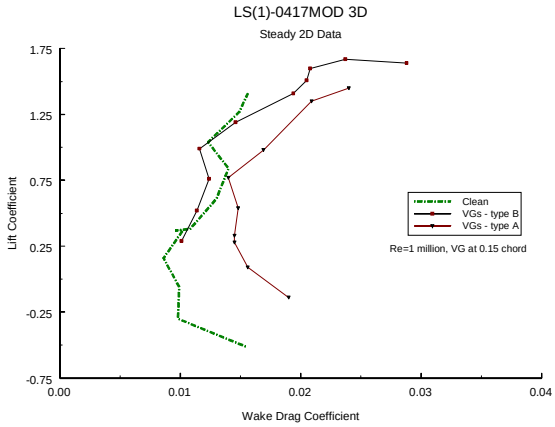

Figure 9. 2D wake drag coefficient with vortex generators.

The type B vortex generators gave very little increase in wake drag over the clean airfoil as seen in figure 9. In comparison type A increased the zero lift drag by approximately 50%.

Unsteady 2D Data

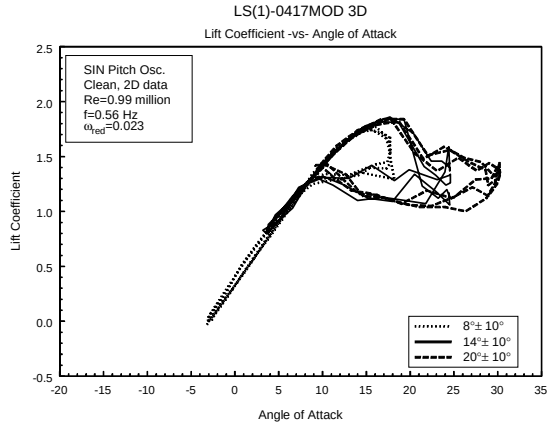

Figure 10. Clean unsteady 2D data.

In comparison with the steady state, the unsteady tests showed higher maximum lift coefficients for both clean and with LEGR applied. Figure 10 shows the clean lift coefficient for the reduced frequency of 0.023. The reduced frequency is defined by equation 1.

$$\omega_{red} = \frac{\pi f c}{U_{\infty}} \qquad (1)$$

The maximum lift coefficient is 1.86, while the downswing lift falls to 1.07. This large difference in the lift coefficient shows greater hysteresis effects with the higher amplitude oscillations of ± 10˚. For the lower

amplitude of ±5.5˚, the hysteresis is not so pronounced especially for the 8˚ mean angle, as shown in Figure 11.

Also the lower amplitudes did not produce such high maximum lift coefficients as the higher amplitudes. The maximum lift coefficient is 1.86 and the down-swing lift 1.3 (30% lower). Also the hysteresis behavior becomes

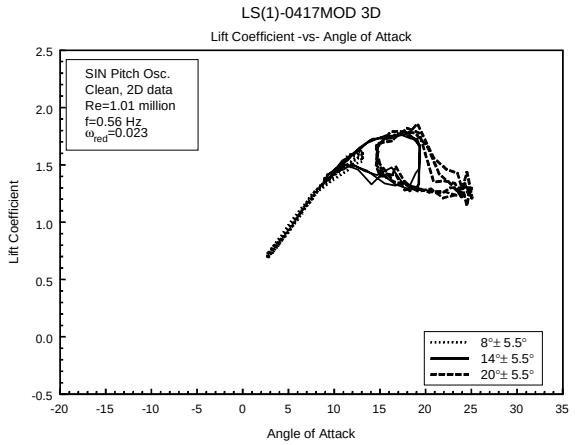

Figure 11. Clean unsteady 2D data for low amplitude.

more pronounced at higher frequencies for both ± 5.5˚ and ± 10˚ cams. The moment coefficients exhibit negligible hysteresis behavior.

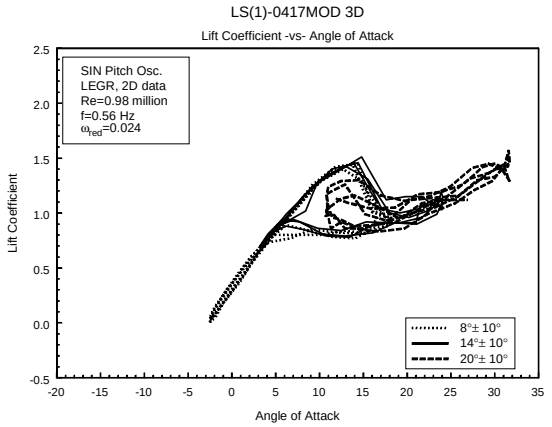

Figure 12. LEGR applied unsteady 2D data.

The application of the LEGR, as in steady state, causes a reduction in the maximum lift coefficients. It also increases the hysteresis loops, especially for the lower mean angles. In Figure 12 the maximum lift coefficient for ± 10˚ cam decreased to 1.57 for the LEGR applied case from 1.86 for the clean case. The downswing lift coefficient was much lower and the loop persisted into lower angles of attack. This behavior is especially visible at the higher frequency of 1.8 Hz, as seen from Figure 13.

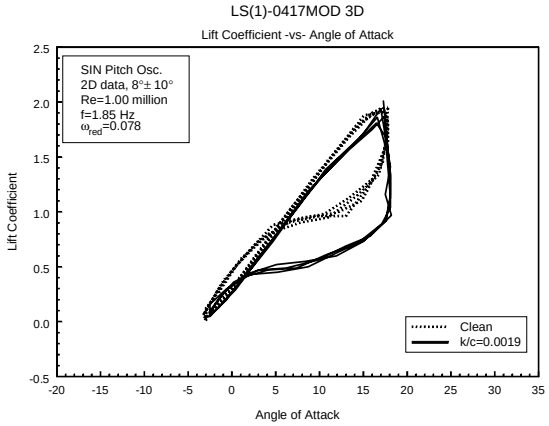

Figure 13. Comparison of clean and LEGR applied.

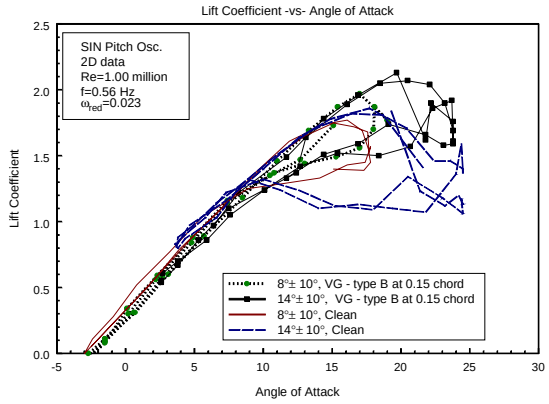

Figure 14. Low frequency ±10˚ oscillation data with vortex generators.

Unsteady flow data with the application of vortex generators are shown in figures 14 and 15 for the low frequency and high frequency cases, respectively. At the low frequency for the ± 10˚ oscillations, type B vortex generators produced higher lift and also made the hysteresis loop smaller for both the 8˚ and 14˚ mean angles. The hysteresis loop with the clean model can persist into low angles of attack, while with the vortex generators applied, the lift coefficient on the downswing is much higher. A slight shift in the lift curve slope also occurs.

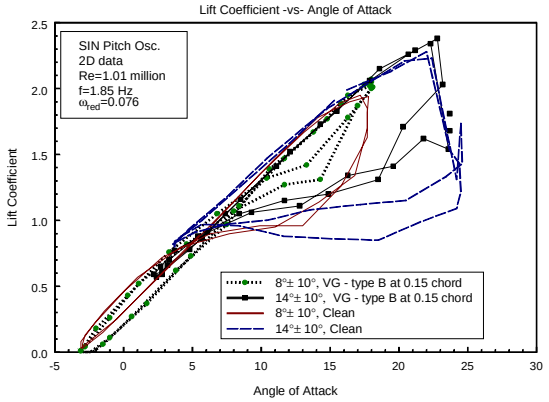

Figure 15. High frequency ±10˚ oscillation with vortex generators.

At the higher frequency, the effects are even more pronounced, as seen in figure 15. The vortex generators in this case produce little effect on the maximum lift coefficient but the hysteresis loops become smaller. With the vortex generators the hysteresis loop at 8˚ mean angle is approximately half size of the clean one. The return offset at low angles of attack is slightly larger and a minor shift of the lift curve slope occurs.

Steady 3D Data

In this configuration the model had a semispan of 76 cm (30 in), therefore an aspect ratio of 3.3. For clarity, data from only 2 spanwise stations (z=0.075 and z=0.925) are shown although the data were acquired at all 6 stations. The characteristic lift coefficient "fan" for a finite wing due to the influence of the vortex system can be seen for both clean and LEGR applied data in figure 16 and figure 17, respectively.

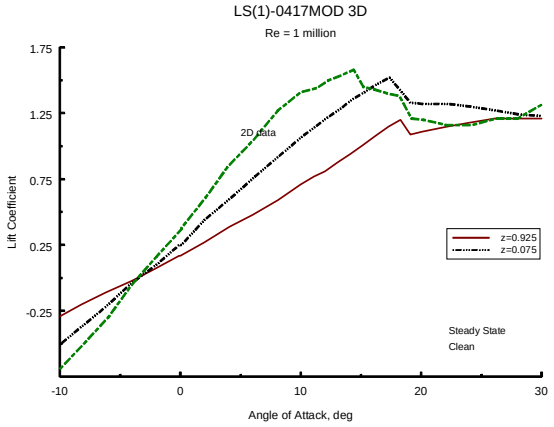

Figure 16. Comparison of 3D steady state clean lift coefficient.

The maximum lift coefficient for the 3D cases drops from the 2D value drastically, also the angle of attack at which the maximum lift coefficient occurs increases for 3D. The maximum lift coefficient for 2D is 1.58 at 14.4˚ angle of attack but for 3D z=0.075 (wall station) is 1.58 at 19.5˚ and for z=0.925 (tip station) the maximum lift coefficient is 1.2 at 18.3˚. The lift curve slope changed from 0.113 clean 2D to 0.080 for z=0.075 (wall) and 0.053 for z=0.925 (tip).

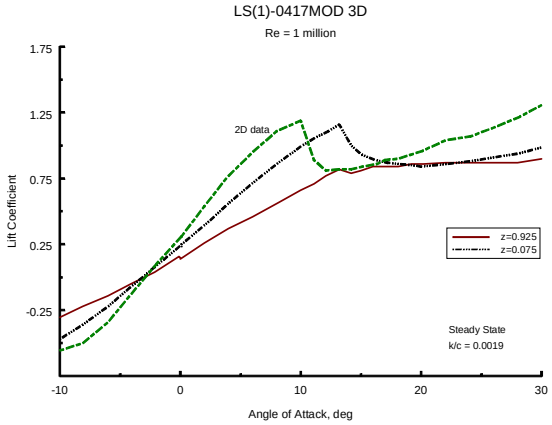

Figure 17. Comparison of 3D steady state LEGR applied lift coefficient

As seen in figure 17, the LEGR applied case produces the same characteristics as for the clean model, except in the region after stall were the lift coefficients are more regular. As usual with the application of LEGR, the maximum lift coefficient drops approximately 30% from the 3D LEGR applied case.

The pitching moment coefficients are, again, essentially unchanged from those of 2D from -10˚ to 10˚ for both the clean and LEGR applied cases.

Many other parameters and correlation values can be calculated from these data. For example, the induced angle of attack (i.e. the difference in the freestream (2D) flow direction and the local 3D flow direction). For both clean and LEGR applied data the induced angle of attack increases with the geometric angle of attack and span location. The application of the LEGR lowers the induced angle of attack for all span location and geometric angle of attack in comparison with the clean data.

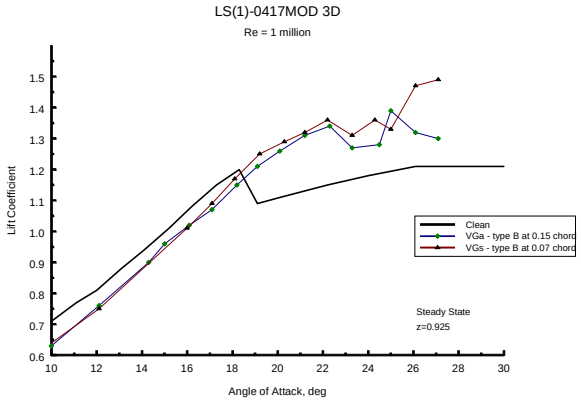

Figure 18. Tip station in 3D configuration with vortex generators.

The application of vortex generators caused dramatic effects on the wing (3D) characteristics. The lift curve slope is shifted by 0.05. For the tip location (z=0.925), shown in figure 18, the lift coefficient increases quite extensively for both positions of the vortex generators at 0.07chord and 0.15 chord. The vortex generators at 0.07 chord gave slightly better results than those located further aft. The clean maximum lift coefficient of 1.2 was obtained at 18˚, while with the vortex generators, stall was delayed to 22˚ and maximum lift coefficient was increased to 1.36.

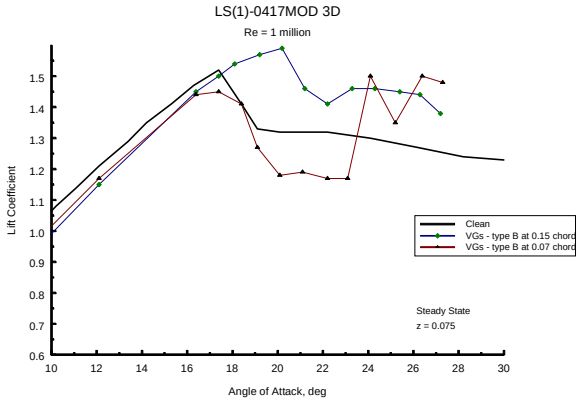

Figure 19. Wall station in 3D configuration with vortex generators.

Figure 19 shows that the 3D clean maximum lift coefficient was 1.52 at 17˚, while with the application of the vortex generators at 0.07 chord the maximum lift coefficient dropped lower than the clean case and stall occurred earlier. When the vortex generators were moved further aft to 0.15, the maximum lift coefficient increased to 1.58 at 20˚.

Unsteady 3D Data

In general, as with the 2D data, the maximum lift coefficient has increased beyond the steady state value but it did not exceed the 2D value. The attack angle for the maximum lift coefficient has increased up to 30˚, well beyond that of steady state. The characteristics of the 3D data have not changed much from the 2D. The lift hysteresis loop for the tip location (z=0.925), is small and increases closer to the wall. The upswing and return-swing data for the 3D configuration are almost identical for the low angles of attack. However, the 2D case shows a "offset", with the lift coefficients being slightly higher on the return-swing.

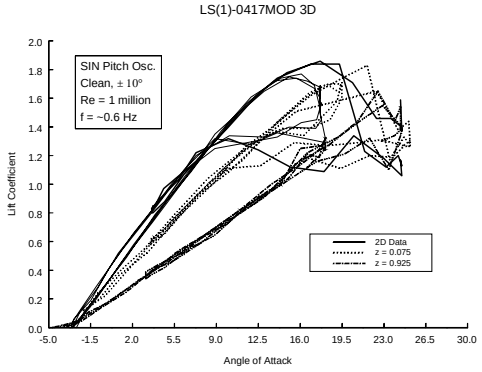

Figure 20. 3D Clean, C_l vs α, $\pm$ 10˚, ω_{red}~0.022.

At the low reduced frequency (0.022) for clean model condition at the span locations of 0.075 (wall) and 0.925 (tip), the data are shown in figure 20, with the 2D data having been added for comparison. For z=0.075 the maximum lift coefficient is 1.92 at angle of attack of 21.9˚ compared with the steady state at 1.52 at 17.4˚ (26% increase); the 2D value was 1.86 at 17.7˚ and the 2D steady state 1.58 at 14.4˚ (only a 17% change). For the tip location of 0.925, also in figure 20, the maximum lift coefficient is 1.65 at 22.5˚. A 37% increase in lift coefficient occurs comparing with the steady state lift coefficient of 1.20 at angle of attack of 18.3˚.

Figure 21 contains the data for the (highest) reduced frequency of 0.077, clean model condition. As before, the

highest lift coefficient occurs for the 2D model configuration and the lowest lift coefficient is at the tip of the 3D model. For the z=0.075 the maximum lift coefficient is 2.26 at 26.8˚; previously noted the steady state maximum lift coefficient was 1.52 at 17.4˚ (a 49% increase). For the z=0.925 the maximum lift coefficient occurred at 28.0˚ and was 2.04, (steady state value was 1.20) a 70% increase. The 2D model configuration showed an increase of 60% in the maximum lift coefficient.

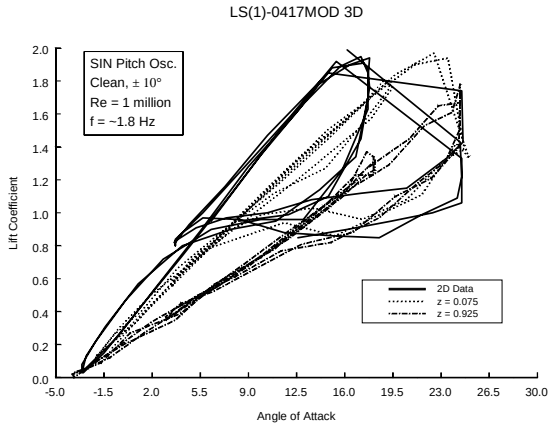

Figure 21. 3D clean, C_l vs α, ±10˚, ω_{red}~0.077.

The quarter chord pitching moment for all span locations falls almost exactly within the same range as the 2D data. A slight variation is seen at low angles of attack where the 2D case has a slightly more negative moment.

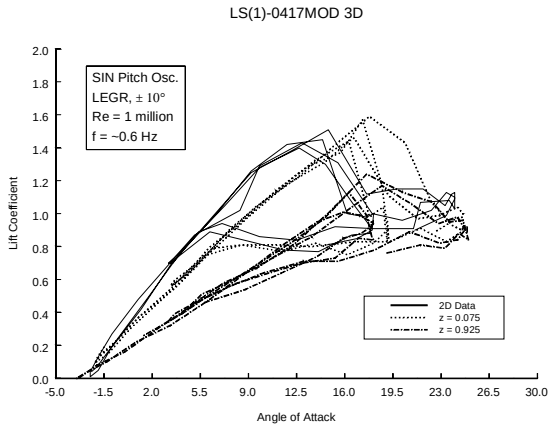

Figure 22. 3D k/c=0.0019, C_l vs α, ±10˚, ω_{red}~0.022.

The application of the LEGR produces a lower maximum lift coefficient and more dramatic stall characteristics especially in the 2D data and span locations closer to the wall. The tip span location (z=0.925) does not have the same characteristics, it is more similar in shape to the clean data. For the low reduced frequency case (0.022) with the LEGR applied, shown in figure 22, the maximum lift coefficient for z= 0.075 is 1.62 at 17.9˚; it is actually higher than the 2D case, which achieved a maximum lift coefficient of 1.51 at 14.8˚. In comparison with the steady state (1.19 at 20.0˚) the maximum lift coefficient increase 40% for z =0.075. The maximum lift coefficient for z = 0.925 is 1.25 at19.2˚ in comparison with the steady state value of 0.82 at 13.2˚, (a 52% increase). In the low reduced frequency cases for both clean and LEGR applied the increase in the maximum lift coefficient varies with the span location, such that the wall position has the smallest change and the tip the highest; 2D data show the lowest maximum lift coefficient increase.

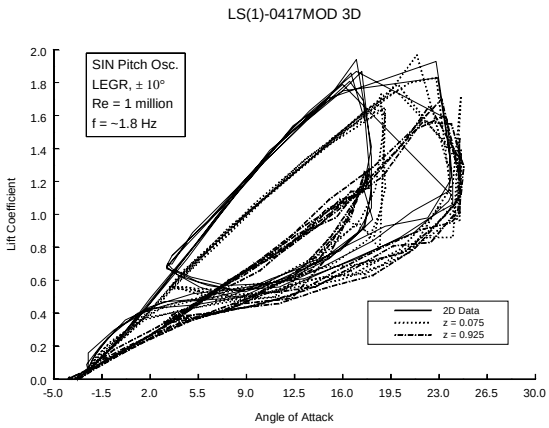

Figure 23. 3D k/c=0.0019, C_l vs. α, ±10˚, ω_{red}~0.077.

Now looking at the high frequency case (.077), shown in figures 23, the hysteresis loop for the lift coefficient narrows as the tip of the model is approached. The 2D case exhibits the larger loop. As before the maximum lift coefficient moves to higher angles of attack for sections close to the tip. The maximum lift coefficient for z =0.075 is 2.19 at 23.1˚ (a 89% increase in comparison with steady state), for z=0.925 the lift coefficient increased to 2.04 (28.0˚) from the steady state of 0.82 (149% increase). For the 2D the maximum lift coefficient is 2.25, 89% higher than the steady state. The 2D data obtained the highest lift coefficients, since it has no tip vortex, which by inducing the additional flow changes the characteristics of the lift.

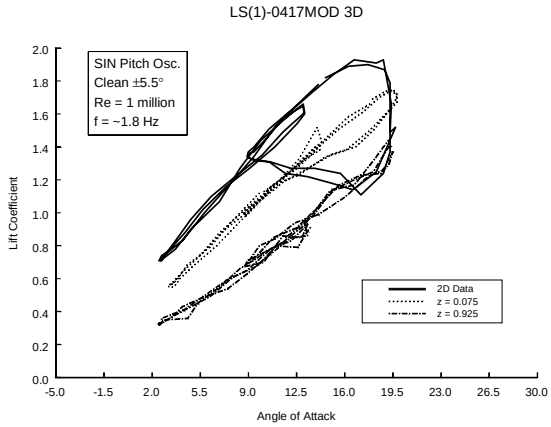

Figure 24. 3D clean, C_l vs α, ±5.5˚, ω_{red}~0.077.

The effects of the application of the LEGR are most noticeable in the lower amplitude oscillations, ±5.5˚. As an example, figure 24 contains the data for the reduced frequency of 0.077, clean model condition and figure 25 for the LEGR applied case. For the z=0.075(wall) the maximum lift coefficient is 2.05 at 24.0˚; previously noted the steady state maximum lift coefficient was 1.52 at 17.4˚ (a 34% increase). For the z=0.925(tip) the maximum lift coefficient occurred at 24.4˚ and was 1.83, a 53% increase.

Now looking at the high frequency case, shown in figures 25, the hysteresis loop for the lift coefficient narrows as the tip of the model is approached; the 2D case exhibits the larger loop, which is true for all frequencies. As before the maximum lift coefficient moves to higher angles of attack for sections closer to the tip. The maximum lift coefficient for z =0.075 is 1.68 at 18.8˚ (a 45% increase in comparison with steady state), for z=0.925 the lift coefficient increased to 1.38 (18.9˚) from the steady state value of 0.82 (68% increase).

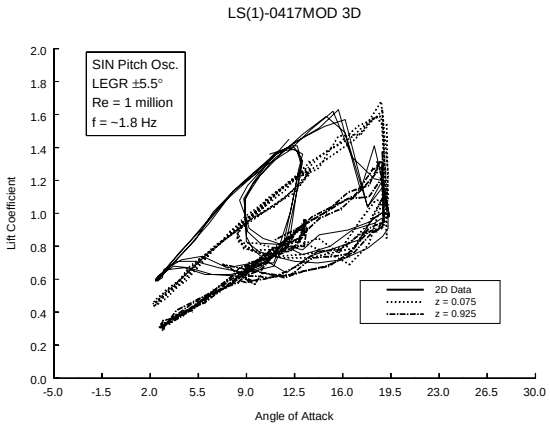

Figure 25. 3D k/c=0.0019, C_l vs. α, ±5.5˚, ω_{red}~0.077.

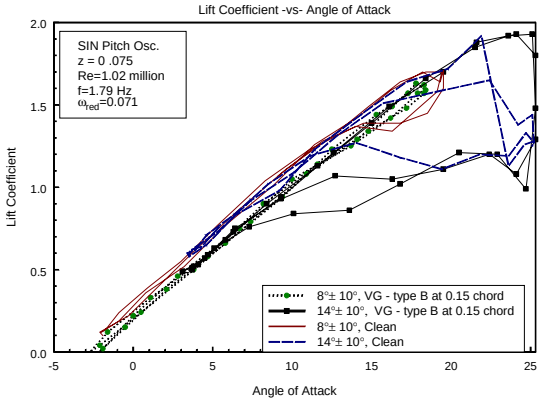

Figure 26. 3D with vortex generators.

While the vortex generators applied at 0.07 or 0.15 chord increase the maximum lift coefficient for the steady state, they have little effect on the oscillating cases. Some increase in maximum lift coefficient is visible in the wall station as seen in figure 26.

CONCLUSIONS

The LS(1)-0417MOD airfoil model in 2D configuration had a maximum lift coefficient of 1.58 at 14.4˚ for 1 million Reynolds number. The application of the LEGR reduced the maximum lift by approximately 50% and increased the minimum drag coefficient by 75%. The application of the vortex generators increases the maximum lift coefficient by 15%.

The unsteady 2D maximum lift coefficient and the hysteresis loops increased with the reduced frequency.

The maximum lift coefficient was up to 186% higher than the steady state. The application of the LEGR reduced the lift by 9% to 30% depending on the amplitude of the oscillations. As mentioned earlier, the hysteresis loop with LEGR persisted into lower angles of attack. The application of the vortex generators increased the lift coefficient by only 10% and also decreased the size of the hysteresis loops.

In the 3D configuration the lift increases as the span station decreases. The maximum pre-stall lift coefficient decreased with the application of the LEGR 21 to 32%. The angle of attack at stall decreases from an average 18.5˚ to 13.9˚. There is little change between the clean and LEGR applied lift curve slopes at the same stations.

The application of the vortex generators made dramatic changes in the lift coefficient in 3D especially at the z=0.075 station. It was found that the vortex generators have to be located further aft closer to the wall and more forwards at the tip. The vortex generators increased the maximum lift coefficient and maintained it for more than 5˚ past the onset of stall.

The higher maximum lift coefficient occurred at z=0.075, which is closest to the wall where the flow resembles 2D the most. The maximum lift coefficient was up to 50% higher than the corresponding steady state. The application of the LEGR reduced the maximum lift coefficient up to 20%. The reduction is much less than for the 2D cases. The vortex generators had only slight benefits on the unsteady 3D flow field.

ACKNOWLEDGMENTS

This work was supported by the National Renewable Energy Laboratory under contract number XAM-7-17203-1.

REFERENCES

[1] Janiszewska, J.M. and Gregorek, G.M., "Two Dimensional and Three Dimensional Flow Characteristics of a LS(1)-0417 MOD Airfoil Model with Applied Grit Roughness and Pitch Oscillations," Submitted to National Renewable Energy Laboratory, Golden, CO.

[2] Fuglsang, Peter and Bak, Christian, 2001,"Design and Verification of the New Risø-A1 Airfoil Family for Wind Turbines," 2001 ASME Wind Energy Symposium, Reno, NV, pp81-91, AIAA-2001-0028.

[3] Lin, J.C., 1999, "Control of Turbulent Boundary-Layer Separation Using Micro-Vortex Generators," 30th AIAA Fluid Dynamics Conference, Norfolk, VA, AIAA 99-3404.

[4] Kerho, M., Hutcherson, S., Blackwelder, R.F., and Liebeck, R.H., 1993, "Vortex Generators Used to Control Laminar Separation Bubbles," Journal fo Aircraft, Vol. 30, No. 3, pp. 315-319.

[5] Dommasch, D., Sherby, S., et-al, 1961, "Airplane Aerodynamics," New York, NY, Pitman Publishing Corp.